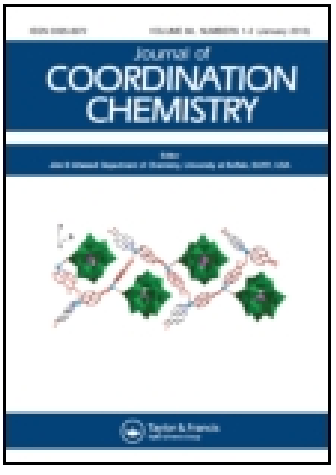

Journal of Coordination Chemistry
Publication details, including instructions for authors and subscription information:
http://www.tandfonline.com/loi/gcoo20

Synthesis, structure, magnetism and antibacterial properties of a 2-D nickel(II) metal-organic framework based on 3-nitrophthalic acid and 4,4′-bipyridine

Xinyi Lu[a], Junwei Ye[a], Limei Zhao[a], Yuan Lin[a] & Guiling Ning[a]
[a] State Key Laboratory of Fine Chemicals and School of Chemical Engineering, Faculty of Chemical, Environmental and Biological Science and Technology, Dalian University of Technology, Dalian, PR China

Accepted author version posted online: 07 Apr 2014.Published online: 30 Apr 2014.

To cite this article: Xinyi Lu, Junwei Ye, Limei Zhao, Yuan Lin & Guiling Ning (2014) Synthesis, structure, magnetism and antibacterial properties of a 2-D nickel(II) metal-organic framework based on 3-nitrophthalic acid and 4,4′-bipyridine, Journal of Coordination Chemistry, 67:7, 1133-1140, DOI: 10.1080/00958972.2014.910773

To link to this article: http://dx.doi.org/10.1080/00958972.2014.910773

Journal of Coordination Chemistry, 2014
Vol. 67, No. 7, 1133–1140, http://dx.doi.org/10.1080/00958972.2014.910773

Synthesis, structure, magnetism and antibacterial properties of a 2-D nickel(II) metal–organic framework based on 3-nitrophthalic acid and 4,4′-bipyridine

XINYI LU, JUNWEI YE*, LIMEI ZHAO, YUAN LIN and GUILING NING*

State Key Laboratory of Fine Chemicals and School of Chemical Engineering, Faculty of Chemical, Environmental and Biological Science and Technology, Dalian University of Technology, Dalian, PR China

(*Received 1 November 2013; accepted 11 February 2014*)

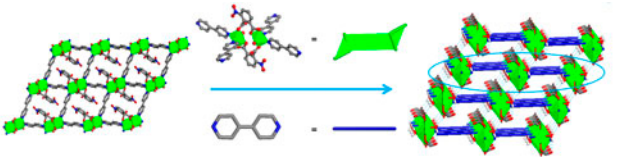

A 2-D nickel(II) mixed-ligand metal–organic framework $[Ni(NPTA)(4,4'\text{-bipy})(H_2O)]_n$ (**1**) was synthesized by reaction of 3-nitrophthalic acid (H_2NPTA) and 4,4′-bipyridine (4,4′-bipy) with Ni(II) under hydrothermal condition and characterized by elemental analysis, infrared spectroscopy, and single-crystal X-ray diffraction analysis. Compound **1** possesses a 2-D layer structure constructed from dinuclear nickel(II) building blocks in which two crystallographically equivalent Ni ions are bridged by two NPTA ligands. Furthermore, the layers are connected into 3-D supramolecular network by hydrogen bonds. The magnetism and antibacterial activity of **1** were investigated.

Keywords: Metal–organic framework; Nickel; Dinuclear building blocks; Magnetic property; Antibacterial activity

1. Introduction

Metal–organic frameworks (MOFs) have attracted interest in chemistry and material science owing to structural diversity and promising applications in gas storage, absorption, catalysis, ion exchange, optics, and magnetic materials [1–3]. A number of MOFs have been synthesized via a powerful strategy of molecular building blocks (MBBs), in which metal ions or metal clusters act as nodes and ligands act as linkers [4]. Among the various transition metal-based MOFs obtained so far, Ni-based MOFs are particularly worth investigating owing to advantages in magnetism and catalysis [5]. Bacterial applications of Ni-based

*Corresponding authors. Email: junweiye@dlut.edu.cn (J. Ye); ninggl@dlut.edu.cn (G. Ning)

MOFs have rarely been explored. The design and synthesis of Ni-based MOFs with desired structures still remains a challenge because assembly of structures is influenced by reaction temperature, solvent, pH, etc. [6, 7]. Based on our previous study, 5-nitroisophthalic acid (H_2NIPH) is a versatile ligand to build MOFs owing to flexibility of coordination modes [8]. As a continuation of this work, 3-nitrophthalic acid (H_2NPTA) was selected to construct functional MOFs because of various coordination modes like H_2NIPH but with different substituent position of carboxylic and nitro groups. Some transition metal complexes based on H_2NPTA have been obtained previously [9–11], however, Ni-based complexes with H_2NPTA have been less reported [12].

In this article, we report the hydrothermal synthesis of a 2-D Ni-based MOF, [Ni(NPTA)(4,4′-bipy)(H_2O)]$_n$ (**1**), based on 3-nitrophthalic acid (H_2NPTA) and 4,4′-bipyridine (4,4′-bipy) as ligands. The crystal structures, thermogravimetric, magnetic, and antibacterial properties of **1** are also presented.

2. Experimental

2.1. *Materials and instruments*

All reagents were of reagent grade and used without purification. Elemental analysis was performed on a Perkin-Elmer 240C elemental analyzer. FT-IR spectra were recorded on a Bruker IFS 66 V interferometer. Thermogravimetric analysis (TGA) was performed on a Perkin-Elmer TGA 7 unit with a heating rate of 10 °C min^{-1}. The as-prepared samples were characterized by XRD (Rigaku-DMax 2400) in reflection mode (Cu Kα radiation) at scanning rate of 0.02 S-1 of 2θ from 5° to 35°. The magnetism was characterized by Quantum Design SQUID magnetometer (MPMS-XL).

2.2. *Synthesis of single crystal [Ni(NPTA)(4,4'-bipy)(H_2O)]$_n$ (1)*

A mixture of $Ni(NO_3)_2$ (0.6 mM), H_2NPTA (0.6 mM), 4,4′-bipy (0.6 mM), and water (10 mL) was stirred for 30 min and sealed in a 25 mL Teflon-lined stainless steel autoclave at 120 °C for 3 days. After cooling to room temperature, green block-shaped crystals were obtained. The yield was 42% based on Ni. Element Anal. Calcd (%) for [Ni(NPTA)(4,4′-bipy)(H_2O)]$_n$: C, 49.87; H, 2.94; N, 9.50. Found: C, 50.05; H, 2.96; N, 9.88. IR (KBr, cm^{-1}) data: 3264, 3093, 1604, 1559, 1466, 1389, 1345, 1215, 1071, 930, 819, 724, 633, 430.

2.3. *Single-crystal X-ray crystallography*

The crystal structure of **1** was determined by single-crystal X-ray diffraction. The reflection data were collected on a Rigaku R-AXIS RAPID diffractometer (Mo Kα radiation, graphite monochromated). Empirical absorption correction was applied for all data. The structure was solved by direct methods and refined by full-matrix least-squares on F^2 using SHELXTL97 software [13]. The heaviest atoms were first found. O, N, and C were subsequently located in difference Fourier maps. All non-hydrogen atoms were refined anisotropically. Hydrogens were calculated by geometrical models. Experimental details for structure

Table 1. Crystallographic data and structure refinement for **1**.

Empirical formula	$C_{18}H_{13}N_3O_7Ni$
Formula weight	442.00
Crystal system	Triclinic
Space group	*P-1*
a (Å)	8.6229(19)
b (Å)	10.968(3)
c (Å)	11.520(3)
α (°)	105.517(16)
β (°)	107.985(14)
γ (°)	108.104(13)
Volume (Å^3)	901.9(4)
Z	2
D_{Calcd} (mg/m^{-3})	1.628
μ (mm^{-1})	1.125
F (0 0 0)	452
R_{int}	0.0386
GOF on F^2	1.412
R_1 $[I > 2\sigma(I)]$*	0.0670
wR_2 $[I > 2\sigma(I)]$*	0.2129
R_1 (all data)*	0.0822
wR_2 (all data)*	0.2205

*$R_1 = \Sigma||F_o| - |F_c||/\Sigma|F_o|$; $wR_2 = \{\Sigma[w(F_o^2 - F_c^2)^2]/\Sigma[w(F_o^2)]^2\}^{1/2}$.

Table 2. Selected bond lengths [Å] and angles [°] for **1**.

$[Ni(NPTA)(4,4'\text{-bipy})(H_2O)]_n$			
Ni(1)–O(3)$^{\#1}$	2.054(4)	Ni(1)–N(1)	2.086(6)
Ni(1)–O(7)	2.057(5)	Ni(1)–O(2)	2.138(4)
Ni(1)–N(2)	2.081(5)	Ni(1)–O(1)	2.165(4)
O(3)$^{\#1}$–Ni(1)–O(7)	92.7(2)	O(7)–Ni(1)–O(1)	88.6(2)
O(3)$^{\#1}$–Ni(1)–N(2)	95.0(2)	N(2)–Ni(1)–O(1)	99.5(2)
O(7)–Ni(1)–N(2)	93.8(2)	N(1)–Ni(1)–O(1)	90.01(19)
O(3)$^{\#1}$–Ni(1)–N(1)	86.1(2)	O(2)–Ni(1)–O(1)	61.66(16)
O(7)–Ni(1)–N(1)	169.7(2)	O(3)$^{\#1}$–Ni(1)–C(7)	134.1(2)
N(2)–Ni(1)–N(1)	96.5(2)	O(7)–Ni(1)–C(7)	87.2(2)
O(3)$^{\#1}$–Ni(1)–O(2)	103.78(17)	N(2)–Ni(1)–C(7)	130.8(2)
O(7)–Ni(1)–O(2)	85.13(18)	N(1)–Ni(1)–C(7)	86.3(2)
N(2)–Ni(1)–O(2)	161.17(19)	O(2)–Ni(1)–C(7)	30.44(19)
N(1)–Ni(1)–O(2)	85.20(19)	O(1)–Ni(1)–C(7)	31.24(19)
O(3)$^{\#1}$–Ni(1)–O(1)	165.24(17)		

Note: Symmetry transformations used to generate equivalent atoms: $^{\#1}$ $-x+2, -y, -z+1$.

analysis are given in table 1. Selected bond distances and angles are listed in table 2 and hydrogen bonds are listed in table S1, see online supplemental material at http://dx.doi.org/10.1080/00958972.2014.910773.

2.4. *Zone of inhibition technique*

A stock solution of 100 ppm was made by dispersing **1** in aqueous solution and making it up to the mark with double-distilled water. The medium was made up by dissolving bacteriological agar and LB broth in distilled water. The mixture was autoclaved for 15 min at 121 °C and then dispensed into sterilized Petri dishes, allowed to solidify, and used for

inoculation. The target micro-organism cultures were prepared separately in 100 mL of liquid LB broth medium for activation. Inoculation was done with the help of a micropipette with sterilized tips. Fifty microliters of activated strain was placed onto the surface of an agar plate and spread evenly over the surface by means of a sterile, bent glass rod. Then, the neutral filter having a diameter of 10 mm, infiltrated the compounds solution, was made using a sterilized borer in each plate.

3. Results and discussion

3.1. *Crystal structure*

The asymmetric unit of **1** consists of one crystallographically unique Ni(II), one NPTA, one 4,4′-bipy, and one coordinated water. As shown in figure 1, the geometry around Ni1 can be described as a distorted octahedron, coordinated with four oxygens from two different NPTA ligands, two nitrogens from two different 4,4′-bipy ligands, and one oxygen atom from a water molecule. The Ni–O distances are 2.054(4)–2.165(4) Å and Ni–N distances are 2.081(5)–2.086(6) Å, which are similar to the reported Ni–O and Ni–N bond lengths [14]. NPTA adopts monodentate and chelate coordination mode to connect two nickel ions forming dinuclear structures in **1** (figure S2), i.e. two crystallographically equivalent Ni ions are bridged by two NPTA ligands to give a dinuclear MBB $[Ni_2N_4(H_2O)_2(NPTA)_2]$ with shorter separations of Ni···Ni (5.212 Å) [figure 1(b)]. The 4,4′-bipy bridges adjacent dinuclear MBBs to form a 2-D layer with a 11.549 × 13.864 $Å^2$ windows [figures 2(a) and S3]. Finally, the 3-D supramolecular network is stabilized by interlayer hydrogen bonds O–H···O (O7–H7A···O4 = 2.562 Å, O7–H7B···O1 = 2.720 Å) in which O–H of coordinated water are donors. The layer–layer distance is 10.968 Å, and the packing of molecule in the unit cell is shown in figure 2.

The simulated and experimental XRD patterns of **1** indicate the phase purity of the products (figure S4). Most peak positions of experimental patterns were in agreement with the simulated value generated from the single-crystal structure analysis. The differences in intensity may be due to preferred orientation of the powder samples.

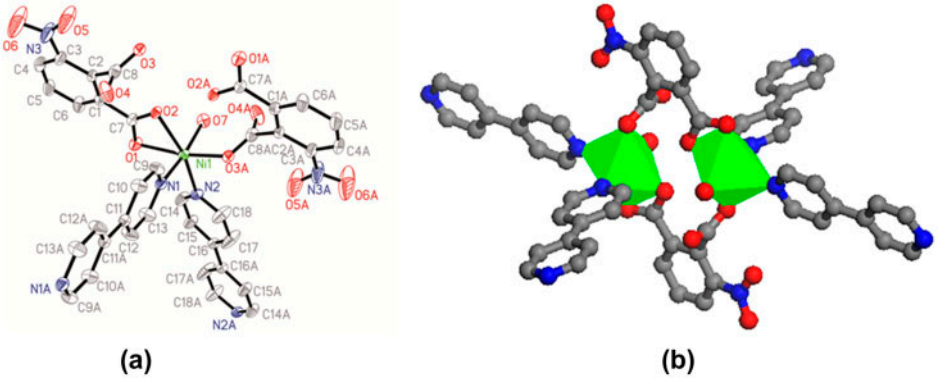

Figure 1. (a) Perspective view of the coordination environment of the Ni centers with 30% thermal ellipsoids; (b) dinuclear building block of Ni center in **1** (color code: Ni green, O red, N blue, C gray, see http://dx.doi.org/10.1080/00958972.2014.910773 for color version).

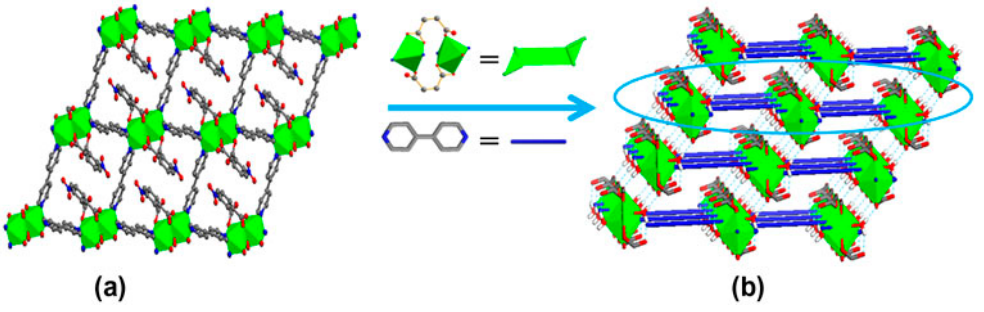

Figure 2. (a) The view of 2-D layers in **1**; (b) 3-D supramolecular network stabilized by interlayer hydrogen bonds in **1**.

3.2. *Thermal stability*

The thermal stability of **1** was examined by TGA (figure 3) under air with a heating rate of 10 °C min^{-1}. Compound **1** loses 4.26% for one coordinated water at 158 °C (Calcd 4.07%). The decomposition of the framework occurred when the temperature is above 285 °C. The remaining product is NiO (14.4%), which is in agreement with the calculated value (16.9%).

3.3. *Antibacterial activity*

Antibacterial study of **1** and H_2NPTA were performed by zone of inhibition technique against Escherichia coli (*E. coli*) and Staphylococcus aureus (*S. aureus*) at 100 ppm. Determination of *in vitro* antimicrobial activity of the metal complex is given in figure 4(a) and the graphical representation is in figure 4(b). About 100 ppm of **1** exhibits antibacterial activity. Compound

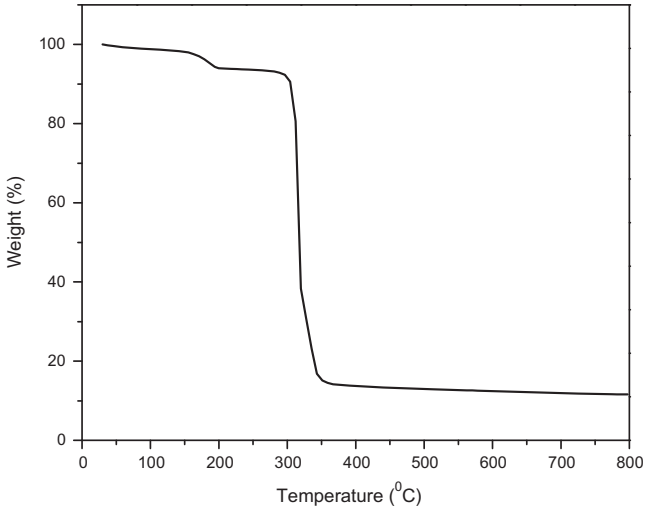

Figure 3. Thermogravimetric curves for **1**.

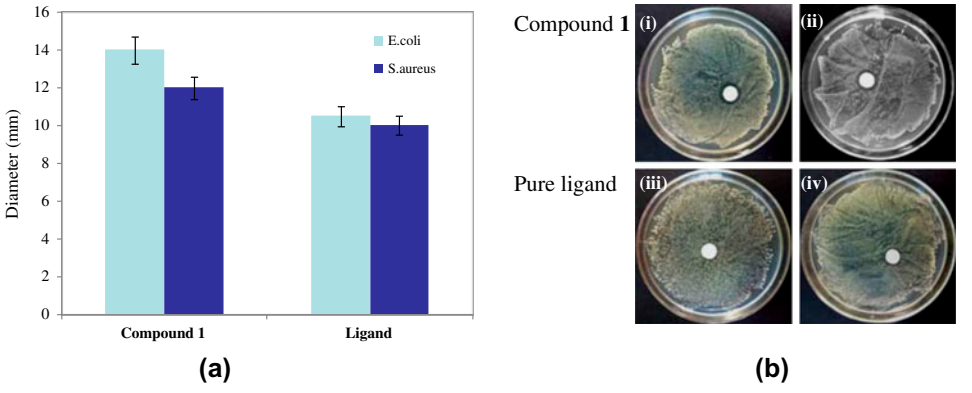

Figure 4. (a) Diameter of inhibition zone technique for **1** and pure ligand against *E. coli* and *S. aureus*; (b) images of inhibition zone for **1** (i, ii) and pure ligand (iii, iv) against *E. coli* and *S. aureus*.

1 has an inhibition zone against *E. coli* of 14 mm, while H_2NPTA is 10 mm. Against *S. aureus*, **1** has a diameter of inhibition of 12 mm, while H_2NPTA is 10 mm. The antibacterial activities of **1** against *E. coli* and *S. aureus* are both higher than that of pure ligand. The antibacterial properties of **1** can be compared with other Ni-based compounds [15] by diameter of inhibition zone. Compared with the inhibition zone of $Ni(H_2L)Cl_2{\cdot}3H_2O$ (H_2L = 2-phenylaminoacetyl-N-phenyl hydrazine carbothioamide) against *S. aureus* in the same concentration [15a], the inhibition zone of **1** is larger. The antibacterial activity for Gram negative bacteria is higher than Gram positive bacteria, which is according to their different cell structures.

3.4. *Magnetism*

Magnetic properties of **1** are characterized by the temperature dependence of the molar magnetic susceptibility χ_M from 2 to 300 K. The temperature dependence of χ_M and $\chi_M T$ for

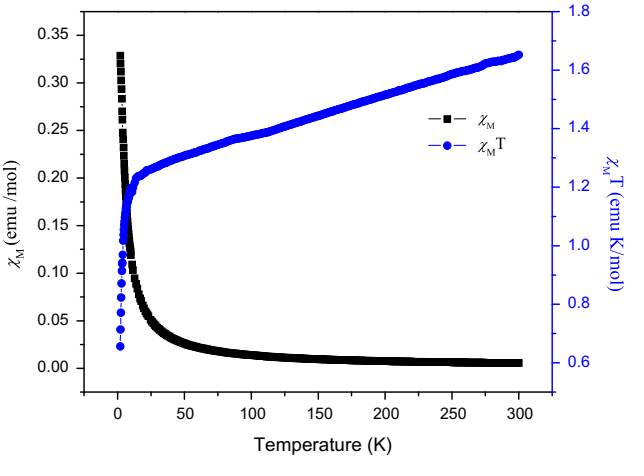

Figure 5. Temperature dependence of $\chi_M T$ and χ_M *vs.* T for **1**.

1 are shown in figure 5. For **1**, $\chi_M T$ monotonously decreases with temperature decrease which demonstrates that antiferromagnetic interactions dominate. The experimental $\chi_M T$ at room temperature is 1.65 emu K M^{-1}, lower than theoretical value (2.65 emu K M^{-1}) for two isolated nickel(II) centers with local spins $S_1 = S_2 = 1$ and $g = 2.3$ [16, 17]. The magnetism of **1** is compared with other Ni-based MOFs. The room temperature $\chi_M T$ value of **1** is higher than reported for dinuclear Ni(II) complexes [18] and mononuclear Ni(II) complexes [19]. With decrease in temperature, $\chi_M T$ decreased to 0.656 emu K M^{-1} at 2 K. It could be presumed that the main magnetic interactions between the Ni(II) centers might happen between the intracluster interaction through the bridging carboxylic group whereas the intercluster interactions through the long 4,4′-bipy can be ignored [20].

4. Conclusion

A new 2-D nickel(II) MOF $[Ni(NPTA)(4,4'\text{-bipy})(H_2O)]_n$ (**1**) was synthesized by a hydrothermal reaction of 3-nitrophthalic acid and 4,4′-bipyridine with Ni(II) salts. Single-crystal X-ray diffraction analysis indicated that **1** is a 2-D layer constructed from dinuclear nickel (II) building blocks, and the layers are connected into a 3-D supramolecular network. Further investigations will focus on the bactericidal mechanism of Ni-based MOFs as disinfectants and tunability of MBBs of MOFs which allow optimization of magnetic and antibacterial properties of MOF materials.

Supplementary material

Crystallographic data for **1** have been deposited at the Cambridge Crystallographic Data Center with the deposition number of CCDC-957447. These data can be obtained free of charge from the Cambridge Crystallographic Data Center via www.ccdc.cam.ac.uk/conts/retrieving.html. Supplementary data associated with this article can be found in the online version.

Funding

This work was supported by National Natural Science Foundation of China [grant number 21076041], [grant number 21276046]; the Ministry of Education, Science and Technology research project; the Fundamental Research Funds for the Central Universities of China.

References

[1] (a) C.N.R. Rao, S. Natarajan, R. Vaidhyanathan. *Angew. Chem., Int. Ed.*, **43**, 1466 (2004); (b) D.J. Tranchemontagne, J.L. Mendoza-Cortés, M. O'Keeffe, O.M. Yaghi. *Chem. Soc. Rev.*, **38**, 1257 (2009); (c) L. Pan, D.H. Olson, L.R. Ciemnolonski, R. Heddy, J. Li. *Angew. Chem., Int. Ed.*, **45**, 616 (2006).

[2] (a) P. Horcajada, C. Serre, G. Maurin, N. A. Ramsahye, F. Balas, M. V. Regí, M. Sebban, F. Taulelle, G. Férey. *J. Am. Chem. Soc.*, **130**, 6774 (2008); (b) A.Y. Robin, K.M. Fromm. *Coord. Chem. Rev.*, **250**, 2127 (2006); (c) B.-L. Chen, S.-C. Xiang, G.-D. Qian. *Acc. Chem. Res.*, **43**, 1115 (2010); (d) O. Kahn, C.J. Martinez. *Science*, **279**, 44 (1998).

[3] (a) X. Du, Y.-L. Sun, B.-E. Tan, Q.-F. Teng, X.-J. Yao, C.-Y. Su, W. Wang. *Chem. Commun.*, **46**, 970 (2010); (b) O.M. Yaghi, G. Li, H. Li. *Nature*, **378**, 703 (1995); (c) Y. Tian, G.D. Li, J.S. Chen. *J. Am. Chem. Soc.*, **125**, 6622 (2003).
[4] (a) O. Sato, T. Iyoda, A. Fujishima, K. Hashimoto. *Science*, **271**, 49 (1996); (b) M.J. Zaworotko. *Nature*, **386**, 220 (1997); (c) D.A. Brown, N.J. Fitzpatrick, H.M. Bunz, A.T. Ryan. *Inorg. Chem.*, **45**, 4497 (2006); (d) S. Polarz, C.L. Pueyo, M. Krumm. *Inorg. Chim. Acta*, **363**, 4148 (2010).
[5] (a) M. Mondelli, V. Bruné, G. Borthagaray, J. Ellena, O.R. Nascimento, C.Q. Leite, A.A. Batista, M.H. Torre. *J. Inorg. Biochem.*, **102**, 285 (2008); (b) C.-L. Ni, Y.-Z. Li, Z.-P. Ni, Q.-J. Meng. *J. Coord. Chem.*, **15**, 1321 (2004); (c) Z. Sun, Y.-S. Ding, L.-J. Tian, X.-T. Zhang. *J. Coord. Chem.*, **66**, 763 (2013); (d) M.-L. Liu, Y.-X. Wang, W. Shi, J.-Z. Cui. *J. Coord. Chem.*, **65**, 1915 (2012); (e) H.-X. Guo, Y.-C. Ke, J.-P. Wang, J. Wu, Z.-S. Zheng. *J. Coord. Chem.*, **65**, 2365 (2012); (f) Y.-L. Chen, J. Yang, J.-F. Ma. *J. Coord. Chem.*, **65**, 3708 (2012).
[6] (a) E.V. Zahínos, F.L. Giles, P.T. García, M.C.F. Calderón. *Eur. J. Med. Chem.*, **46**, 150 (2011); (b) W. Zhao, Y.-L. Qian, J.-L. Huang. *Chin. J. Chem.*, **22**, 732 (2004).
[7] (a) M.V. Angelusiu, S.F. Barbuceanu, C. Draghici, G.L. Almajan. *Eur. J. Med. Chem.*, **45**, 2055 (2010); (b) E.M. Jouad, G. Larcher, M. Allain, A. Riou, G.M. Bouet, M.A. Khan, X.D. Thanh. *J. Inorg. Biochem.*, **86**, 565 (2001).
[8] (a) X.-Y. Lu, J.-W. Ye, W. Li, W.-T. Gong, L.-J. Yang, Y. Lin, G.-L. Ning. *CrystEngComm.*, **14**, 1337 (2012); (b) J.-W. Ye, J.-Y. Zhang, G.-L. Ning, G. Tian, Y. Chen, Y. Wang. *Cryst. Growth Des.*, **8**, 3098 (2008); (c) J.-W. Ye, J.-Y. Zhang, L. Ye, D. Xie, T. Xu, G.-L. Ning. *Dalton Trans.*, 5342 (2008).
[9] (a) X.-J. Zhang, M.-L. Guo. *Acta Crystallogr.*, **E68**, m262 (2012); (b) H.-P. Gao, M.-L. Guo. *Acta Crystallogr.*, **E68**, m264 (2012); (c) H.-X. Guo, Q.-H. Wang, W. Weng, C.-H. Huang, S. L. Lin, M. Jia. *Chin. J. Struct. Chem.*, **26**, 1445 (2007).
[10] (a) Y.-H. Deng, J. Liu, B. Wu, C. Ambrus, T.D. Keene, O. Waldmann, S.-X. Liu, S. Decurtins, X.-J. Yang. *Eur. J. Inorg. Chem.*, **10**, 1712 (2008); (b) X.-L. Wang, B. Mu, H.-Y. Lin, S. Yang, G.-C. Liu, A.-X. Tian, J.-W. Zhang. *Dalton Trans.*, 11074 (2012).
[11] (a) Y.-S. Song, B. Yan, Z.-X. Chen. *Appl. Organomet. Chem.*, **21**, 150 (2007); (b) Y.-F. Han, C. Cheng, S.W. Ng. *Acta Crystallogr. Sect. E*, **66**, m1484 (2010).
[12] (a) J. Zhang, L.-G. Zhu. *CrystEngComm.*, **13**, 553 (2011); (b) J.-M. Shi, J.-Z. Cui, D.-Z. Liao, M.-M. Miao, Y.-J. Liu, Z.-H. Jiang, G.-L. Wang. *Pol. J. Chem.*, **72**, 643 (1998).
[13] G.M. Sheldrick. *SHELXS-97, Program for Crystal Structure Solution*, University of Göttingen, Göttingen (1997).
[14] (a) P. Mukherjee, M.G.B. Drew, C.J.G. García, A. Ghosh. *Inorg. Chem.*, **48**, 5848 (2009); (b) P. Mukherjee, M.G.B. Drew, M. Estrader, A. Ghosh. *Inorg. Chem.*, **47**, 7784 (2008).
[15] (a) S.A. Aly. *J. Chem. Pharm. Res.*, **3**, 1028 (2011); (b) S.G. Wanale, S.P. Pachling. *Res. J. Pharm., Biol. Chem. Sci.*, **3**, 64 (2012).
[16] (a) J.-W. Shin, H.-J. Son, S.-K. Kim, K.-S. Min. *Polyhedron*, **52**, 1206 (2013); (b) R. Biswas, S. Giri, S.K. Saha, A. Ghosh. *Eur. J. Inorg. Chem.*, **17**, 2916 (2012).
[17] J. Ruiz, A.J. Mota, A.R. Diéguez, I. Oyarzabal, J.M. Seco, E. Colacio. *Dalton Trans.*, 14265 (2012).
[18] (a) X.-Q. Shen, Z.-F. Li, H.-Y. Zhang, Z.-J. Li. *J. Coord. Chem.*, **63**, 1720 (2010); (b) A.-J. Lan, L. Chen, D.-Q. Yuan, Y.-G. Huang, M.-C. Hong, X.-T. Wang. *Polyhedron*, **30**, 47 (2011).
[19] X.-J. Li, G.C. Ma, X.-H. Xu. *J. Coord. Chem.*, **66**, 3249 (2013).
[20] (a) C.-Z. Xie, Y.-Z. Liu, Q.-J. Su, Y. Ouyang, J.-Y. Xu. *J. Coord. Chem.*, **63**, 801 (2010); (b) C.-Z. Xie, Q.-J. Su, S.-H. Li, J.-Y. Xu, L.Y. Wang. *Inorg. Chem. Commun.*, **13**, 1476 (2010).